On the Impact of Topology on the Primary Frequency Control of Virtual Power Plants

Weilin Zhong, *Student Member, IEEE*, Taulant Kërçi, *Student Member, IEEE*, Federico Milano, *Fellow, IEEE*
School of Electrical & Electronic Engineering, University College Dublin, Ireland
{weilin.zhong, taulant.kerci}@ucdconnect.ie, federico.milano@ucd.ie

***Abstract*— This paper studies the impact of topology on the primary frequency regulation of Virtual Power Plant (VPP). Two cases are considered, namely, a topology where the Distributed Energy Resources (DERs) that compose the VPP are scattered all-over the transmission grid; and a topology where the DERs are all connected to the same distribution system that is connected to the rest of the transmission grid through a single bus. The case study considers these topologies through modified versions of the WSCC 9-bus system. Detailed models of stochastic disturbances caused by loads, wind speed and solar irradiance, as well as of communication delays of a variety of realistic communication networks are discussed and evaluated.**

***Index Terms*— Virtual Power Plant (VPP), topology, frequency control, Distributed Energy Resource (DER), Energy Storage System (ESS), communication delay.**

I. Introduction

A. Motivation

A Virtual Power Plant (VPP) consists of a cluster of Distributed Energy Resources (DERs) and Energy Storage System (ESS) [1]. Differently to microgrids, the primary goal of VPPs is the generation and they generally do not include nor take into account the network to which the DERs are connected nor the load consumption of such a network. Most studies on the primary frequency support provided by VPPs focus exclusively on the frequency regulation respectively supported by the Solar Photo-Voltaic Generator (SPVG), Wind Generator (WG) or ESS [2]–[4]. The impact on the dynamic performance of the VPP of topology, communication delays due to communication networks and the stochastic variations of loads, wind speed and solar irradiance, on the other hand, have not been thoroughly studied. The paper fills this gap.

B. Literature Review

Similar to conventional generators, the VPP primary frequency control aims to improve the recovery of the frequency to its reference value in short-term transients following a power unbalance. To this aim, DERs and ESSs are integrated and coordinated to provide the frequency containment service.

DERs are the main component of a VPP as they define the capacity of the VPP and allow its participation to the electricity market. The ability of the VPP to provide regulation, in particular frequency containment, rely also on other resources, the most important of which are ESSs. Due to the relatively high cost of ESSs, a coordinated control method for SPVGs and controllable loads that aggregates the power output of the VPP to improve the stability and security of power grids is proposed in [2]. On the other hand, in [3], the electric vehicle (EV) is used as a storage for WG to overcome its uncertainty of generation. Regarding the aggregation of DERs in VPP, reference [5] explores an algorithm to integrate SPVG and WG that smooths the VPP output fluctuation.

ESS is a crucial element of the fast frequency control in the low-inertial system and, in turn, of VPPs. Reference [4] summarizes the requirements for the connection of ESSs as well as their charging and discharging characteristics. The actuation and allocation of ESSs are also important. Reference [6] proposes a novel control algorithm based on historic frequency measurements to allocate ESSs efficiently. The algorithm extends the State of Charge (SoC) limitation of ESS and the application of emergency resistors. Similarly, in [7], it is specified that the islanded and low-inertia systems are more sensitive to power imbalances and suffer greater frequency excursions at such occurrences. In this vein, in [7], the fast-acting ESSs enable the provision of synthetic inertia to mitigate the impact of SPVG and WG on the stability of the grid.

Another crucial element of each VPP is the Energy Management System (EMS). This heavily relies on Information and Communication Technologies (ICT). When a control such as the fast frequency response relies on communication networks, latency and communication delays have to be taken into account as they can have an impact on the dynamic behavior of the VPP as well as of the overall system. This aspect is particularly relevant if the VPP is scattered across the transmission system and the DERs are significantly far away from each other. Reference [8] presents the ICT requirements of VPPs to procure, offer and realize ancillary services. The VPP requirements are then mapped against the services of the extended IEC 61850 standard to enhance the coordination between the VPP service center and DERs. The set up of the communication network in this paper will also follow these requirements.

C. Contributions

The definition of a VPP that also includes the network is sometimes referred to as "technical" VPP or TVPP [1].

This work was supported by Science Foundation Ireland, by funding W. Zhong, Taulant Kërçi and F. Milano under project ESIPP, Grant No. SFI/15/SPP/E3125; and F. Milano under project AMPSAS, Grant No. SFI/15/IA/3074. F. Milano is also supported by the European Commission under project EdgeFLEX, Grant No. 883710.

Nevertheless, as mentioned above, the impact of topology on the frequency control of VPPs has not been investigated so far. This is an important aspect, as indicated in [9], especially for Transmission System Operators (TSOs). Knowing the effect of network constraints, in fact, can provide a guidance on which kind of VPPs topology is more effective in providing a frequency containment service. In turn, this knowledge will help define adequate network codes for the requirements of the frequency control that can be provided by VPPs.

The contributions of this paper are as follows.

- A classification of VPP based on the topology and connection of DERs and ESSs.
- A comprehensive stochastic analysis based on the Monte Carlo method that considers different combinations of topologies and strategies for the primary frequency control of VPPs.
- A discussion of the impact of communication delays on different topologies as well as on the overall dynamic behavior of the system.

D. Organization

The remainder of this paper is organized as follows. Section II describes the frequency control scheme of DERs and ESSs. Section III presents the two types of VPP topologies proposed in the paper. Section IV presents the modeling of the power system with inclusion of stochastic processes and delays. An exhaustive case study based on the WSCC 9-bus system is provided in Section V. Finally, Section VI draws conclusions and outlines future work directions.

II. Primary Frequency Control of VPPs

This section outlines the typical frequency control schemes of the devices that compose a VPP. These are the schemes utilized in the simulations presented in Section V.

Figure 1 depicts a simplified ESS scheme for active power control that aims at regulating a given measured frequency ω with a reference frequency ω^{ref} [10]. The frequency controller is composed of a Proportional-Integral (PI) regulator and a droop controller that couples with the Dead-band (DB) and Low pass filter (LPF), which reduces the sensitivity of the input signal as well as filters out noises, respectively. The scheme in Fig. 1 also represents a storage input limiter to smooth the transients that derive from the energy saturation/exhaustion of the ESS [11]. Then a first-order LPF with capacity limits is used to model the storage device.

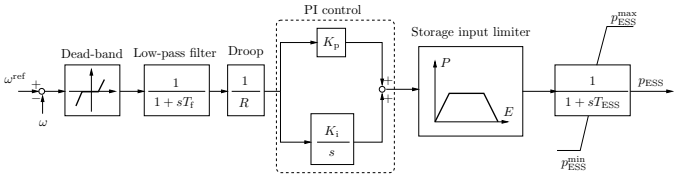

Fig. 1: Typical frequency controller of an ESS.

Figure 2 shows a simple scheme of the frequency controller of SPVGs [12]. The frequency regulation consists of a droop control composed of droop gain and LPF. The output signal is then added to a PI controller with respect to the Maximum Power Point Tracking (MPPT) reference active power signal. Finally, the controller determines the d-axis current of the SPVG converter.

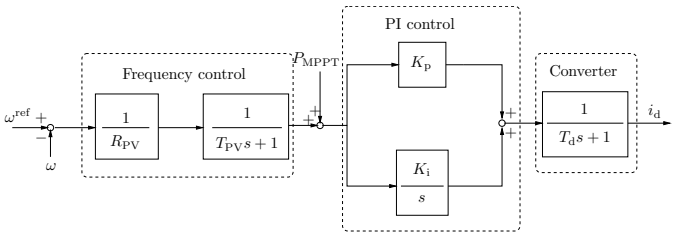

Fig. 2: Typical frequency controller of a SPVG.

Figure 3 shows a typical scheme of the frequency controller of WG that couples the output of the MPPT with the deviation of the frequency [13]. In this case, a frequency control composed of droop control and Rate of Change of Frequency (RoCoF) is introduced. The outputs of the frequency controller then go through a DB and fed the output of the MPPT.

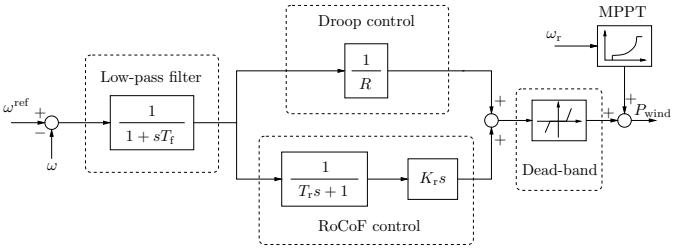

Fig. 3: Typical frequency controller of a WG.

The controllers described so far are independent. In [14], the authors presented a "coordinated" primary frequency control approach of the ESS which combines the DERs active power outputs in VPP. In this control architecture, the VPP provides an extra frequency support following a contingency. With this aim, a feedback signal, p_{co}, that takes into account the difference between the total net active power outputs of DERs (p_{net}) and the VPP active power scheduled for a given period (p_{ref}) is included in the frequency control of the ESS. Figure 4 illustrates the control scheme of the ESS with this coordinated signal. In the case study, we consider the scenario where the signal p_{co} is also included in the frequency controllers of the DERs. That is, the input signal in the schemes of Figs. 2 and 3 is assumed to be $\omega^{\text{ref}} - \omega + p_{\text{co}}$.

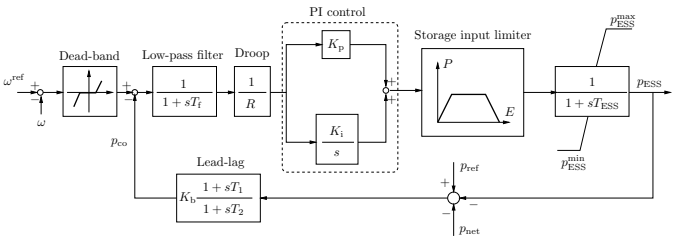

Fig. 4: Primary frequency controller of an ESS belonging to a VPP with inclusion of a coordinated control signal.

III. Topologies

At the system level, two main types of VPP topologies are relevant: (i) transmission system VPP (TS-VPP), where the ESS and DERs are connected directly to the high-voltage Transmission System (TS); and (ii) distribution system VPP (DS-VPP), for which the devices are connected to the TS via a Point of Connection (POC). The TS-VPP topology is widely adopted to combine geographically dispersed and/or high-capacity DERs, whereas the DS-VPP is suitable for the geographically close and small/medium capacity DERs. Figures 5 and 6 illustrate these two topologies.

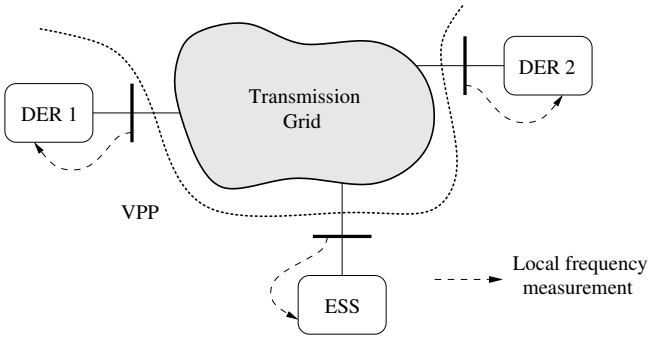

Fig. 5: Illustration of the TS-VPP topology.

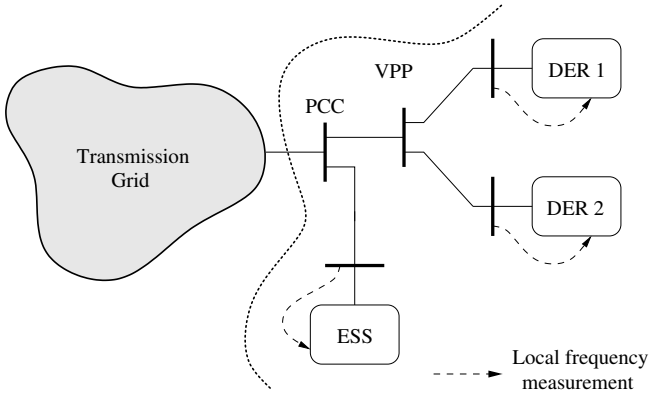

Fig. 6: Illustration of the DS-VPP topology.

IV. Power System Modeling

This section presents a power system model with inclusion of time-variant delays and stochastic processes. Delays allows modeling the latency of the communication network, whereas stochastic processes take into account the volatility of wind speed, solar irradiance and load power consumption.

A. Communication Delays

A communication delay originated by the transmission of remote measurements within a VPP can be modeled as a Wide-Area Communication (WAC) delay [15], [16]:

$$\tau(t) = \tau_f + \tau_p(t) + \theta(t)\,, \tag{1}$$

where τ is the total communication delay, τ_f is the fixed constant delay associated with data measurement and processing, τ_p is the transmission delay, and θ is the associated random jitter that reflects the network issues, e.g. noise, packet losses and background traffic.

The transmission delay in (1) is formulated as:

$$\tau_p = \tau_{po} + \frac{S}{B}\,, \tag{2}$$

where τ_{po} is the propagation delay determined by the transmission medium (e.g. optical fiber, WIFI, or WLAN), S is the packet size of each data, and B is the bandwidth of transmission channel.

In the following, we assume that the delay is included in the signal p_{CO}, as follows:

$$p_{\mathrm{co},d} = p_{\mathrm{co}}\big(t - \tau(t)\big)\,, \tag{3}$$

where $p_{\mathrm{co},d}$ is the delayed VPP output feedback signal.

In this work, the delay due to the communication network is obtained by means of the software tool ns-3 [17], that allows a detailed modeling of communication networks. ns-3 is then interfaced with and co-simulated with the power system software tool Dome [18] as discussed in [19].

B. Stochastic Processes

Stochastic fluctuations are modeled by means of Ornstein-Uhlenbeck processes, which is the solution of the following Stochastic Differential Equation (SDE):

$$\dot{\eta} = a(\eta)\,\eta + b(\eta)\,\xi\,, \tag{4}$$

where a and b are the drift and the diffusion terms of the SDE respectively and ξ represents the white noise, namely the formal time derivative of the Wiener process. Ornstein-Uhlenbeck processes with Gaussian distribution and exponentially-decaying autocorrelation have constant a and b terms. Nonlinear η-dependent a and b term allows defining other probability distributions and behaviors of the autocorrelations [20]. The stochastic models of load, wind, and solar irradiance considered in this paper are based on [21], [22], and [23], respectively. The interested reader can find a detailed description of these stochastic models in the references mentioned above.

C. Power System with Delays and Stochastic Processes

The power system model considered in this paper includes the stochastic processes of wind, solar, and load variations as well as communication delays. The resulting overall system is modeled as the following set of Stochastic Delay Differential-Algebraic Equations (SDDAEs) [21], [24]:

$$\begin{aligned} \dot{\boldsymbol{x}} &= \boldsymbol{f}(\boldsymbol{x}, \boldsymbol{y}, \boldsymbol{y}_d, \boldsymbol{\eta}, \boldsymbol{u})\,, \\ \boldsymbol{0} &= \boldsymbol{g}(\boldsymbol{x}, \boldsymbol{y}, \boldsymbol{y}_d, \boldsymbol{\eta}, \boldsymbol{u})\,, \end{aligned} \tag{5}$$

where $\boldsymbol{f}$ and $\boldsymbol{g}$ are the differential and algebraic equations, respectively; $\boldsymbol{x}$, $\boldsymbol{y}$, $\boldsymbol{y}_d$, $\boldsymbol{\eta}$ and $\boldsymbol{u}$ are the state, algebraic, delayed algebraic, stochastic perturbations and the input variables, respectively.

V. Case Study

The TS-VPP and DS-VPP topologies considered in this paper are both based on a modified version of the well-known WSCC 9-bus, 3-machine system [25].

The setup of the grid for the TS-VPP is shown in Fig. 7. In this scenario, the active and reactive powers of the original load at bus 6 are reduced to 0.578 MW and 0.117 MVAr, respectively. Then, one SPVG, two WGs and one ESS are connected at buses D8, D6, D7, and 9, respectively. The WGs and the SPVG both generate 15 MW at $t = 0$. Finally, the power rate of the ESS is 10 MW.

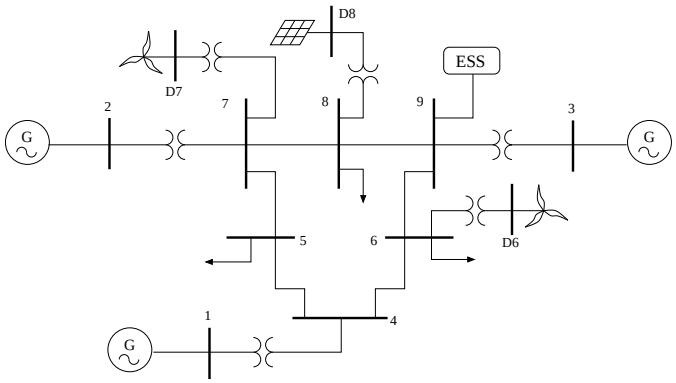

Fig. 7: Modified WSCC 9-bus, 3-machine system with a TS-VPP topology.

The setup of the grid for the DS-VPP is shown in Fig. 8 and consists of the following modifications with respect to the original network.

- The load at bus 6 in the original network is replaced with a Distribution System (DS) that includes a VPP. The DS consists of 8-buses at 38 kV and is connected to the TS through an Under-Load Tap Changer (ULTC) type step down transformer [26].
- The total active and reactive power of the loads in the DS is 0.578 MW and 0.117 MVAr, respectively.
- The VPP includes one SPVG, two WGs, one ESS, with the same parameters as the TS-VPP, that are connected at buses D8, D5, D2, and D2, respectively.

A. Monte Carlo Analysis

This section studies the statistical behavior of the frequency control provided by the TS-VPP and DS-VPP. The study considers both un-coordinated ($K_\mathrm{b} = 0$) and coordinated ($K_\mathrm{b} \neq 0$) frequency controllers as introduced in Section II, as well as the case of VPP without frequency control on DERs and without ESS. The stochastic fluctuations affect 10% of the power consumption of all loads as well as of the wind/solar generated power variations with respect to the forecast of wind speed/solar irradiance. 500 Monte Carlo simulations are carried out for each scenario.

The case study considers both the situations of over and under frequency. With this aim, the following two contingencies are considered: (i) a three-phase fault occurring at bus 5 at $t = 1$ s and cleared after 100 ms by opening the line

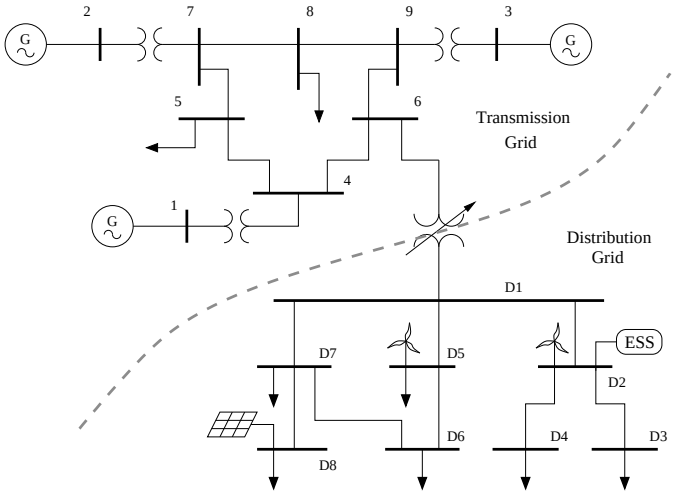

Fig. 8: Modified WSCC 9-bus, 3-machine system with a DS-VPP.

that connects buses 5 and 7; and (ii) a load step increase occurring at $t = 1$ s and corresponding to the 3% of the total loading level of the system. The trajectories of the Center of Inertia (COI) are shown in Figs. 9, 10 and 11. Specifically, Fig. 9 shows the transient behavior of the WSCC system with the VPP but without ESS and frequency control on DERs. Whereas Figs. 10 and 11 show the behavior of the system with inclusion of a VPP with non-coordinated and coordinated, respectively, frequency control of its resources.

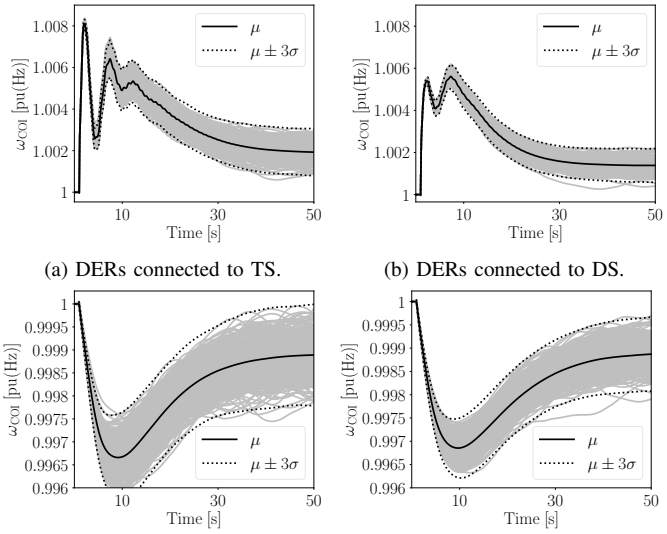

(a) DERs connected to TS. (b) DERs connected to DS.

(c) DERs connected to TS. (d) DERs connected to DS.

Fig. 9: Trajectories of the frequency COI with 500 Monte Carlo simulations for the WSCC 9-bus system with inclusion of DERs without frequency control and without ESS: (a) and (b) three-phase fault; (c) and (d) load increase.

It is interesting to observe, from Fig. 9, that the cases when the DERs are aggregated into a distribution network, i.e. cases (b) and (d), lead to a better dynamic behaviour compared to the cases when DERs are directly connected to the TS, i.e. cases (a) and (c). Furthermore, as expected, the cases with the VPP and without ESS and frequency control on DERs (Fig. 9),

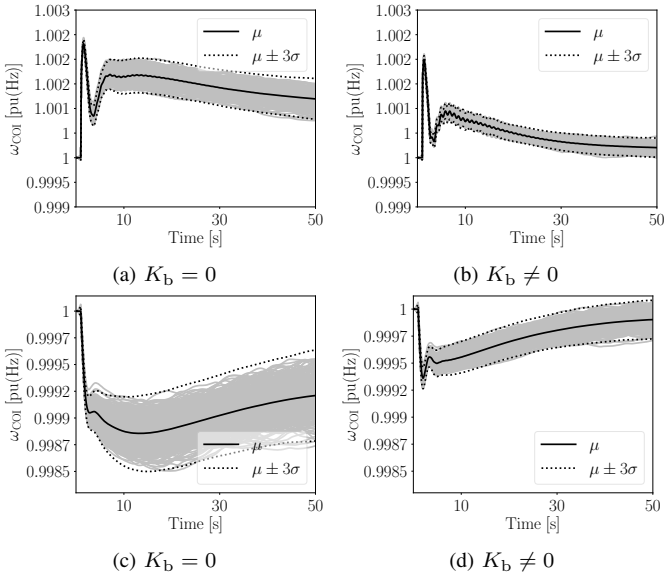

(a) $K_{\mathrm{b}} = 0$ (b) $K_{\mathrm{b}} \neq 0$

(c) $K_{\mathrm{b}} = 0$ (d) $K_{\mathrm{b}} \neq 0$

Fig. 10: Trajectories of the frequency COI with 500 Monte Carlo simulations for the WSCC 9-bus system with inclusion of a TS-VPP: (a) and (b) three-phase fault; (c) and (d) load increase.

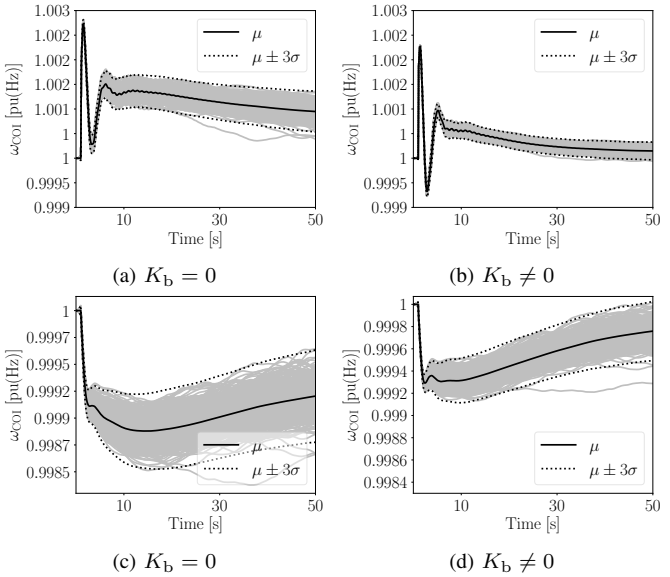

(a) $K_{\mathrm{b}} = 0$ (b) $K_{\mathrm{b}} \neq 0$

(c) $K_{\mathrm{b}} = 0$ (d) $K_{\mathrm{b}} \neq 0$

Fig. 11: Trajectories of the frequency COI with 500 Monte Carlo simulations for the WSCC 9-bus system with inclusion of a DS-VPP: (a) and (b) three-phase fault; (c) and (d) load increase.

leads to higher frequency deviations compared to the cases with inclusion of a VPP with non-coordinated and coordinated frequency control of its resources (Figs. 10 and 11).

With respect to the considered VPP control strategies, the VPP that coordinates the control of DERs and ESSs shows a better frequency transient behavior than the VPP composed of independent devices. With regard to VPP topologies, geographically dispersed DERs and ESSs provide better frequency support to the whole system. In fact, the TS-VPP leads to lower frequency oscillations in the first seconds after the contingency ($0<t<10$ s) and a statisitcally lower spread of the frequency with respect to the DS-VPP (see Table I).

B. Impact of Communication Delays

The impact of communication delays is studied next. To this aim, the communication delay with respect to three levels of communication networks, namely, high-speed, medium-speed, and low-speed communication networks, are introduced. The bandwidth, data rate, and background traffic such as Remote Terminal Unit (RTU) and video stream for each communication network are given in Table II. The detailed setup and parameters of the communication networks can be found in [14]. Table III shows the approximate value of the mean delays in different communication networks. The contingency is the same three-phase fault as Section V-A, and the control approaches of DERs and ESS are coordinated ($K_{\mathrm{b}} \neq 0$) in both TS-VPP and DS-VPP.

Figure 12 shows the trajectories of the impact of communication delays with respect to communication networks with different bandwidths on the system frequency COI. For the TS-VPP, the data transmitted through the geographically dispersed devices give raise to bigger communication delays than for the DS-VPP (see Table III). Simulation results, however, indicate that the DS-VPP is more sensitive to the communication delays than the TS-VPP even if these delays have a smaller magnitude. On the other hand, it is interesting to note that, even if delays are larger, the TS-VPP has a better dynamic performance than the DS-VPP even for the scenario with low-bandwidth communication network. These results indicate that a uniform geographical distributions of the resources of the VPP is beneficial for the regulation of the overall grid and can overcome the deterioration due to the latency of the communication network.

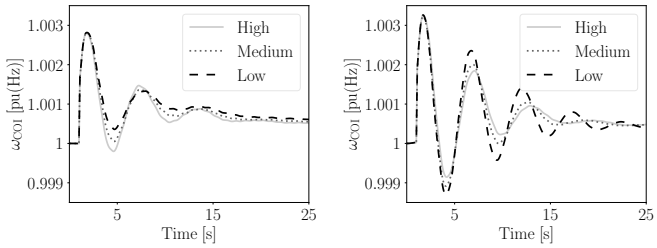

(a) TS-VPP (b) DS-VPP

Fig. 12: Frequency of the COI following a three-phase fault for the 9-bus system with VPP and coordinated resources. The signal p_{co} is transmitted through high/medium/low-bandwidth communication networks, respectively.

VI. Conclusions

The paper compares the performance of VPP primary frequency regulation considering different topologies as well as different frequency control approaches of DERs and ESSs. The impact of communication delays and stochastic disturbances of wind, load, and solar irradiance are also taken into account.

Simulation results indicate that, without proper control, DERs deteriorate the dynamic response of the grid, in particular if they are distributed all-over the transmission grid. Interestingly, the averaging effect of stochastic processes helps reducing the negative impact of DERs if the are located at

TABLE I: Standard deviation of the frequency COI, σ_{COI}. The scenarios corresponds to those indicated in Figs. 9, 10 and 11.

Topology	DERs – no freq. control				TS-VPP				DS-VPP			
Scenario	(a)	(b)	(c)	(d)	(a)	(b)	(c)	(d)	(a)	(b)	(c)	(d)
$\sigma_{\mathrm{COI}} \times 10^{-5}$ [pu(Hz)]	37.8	26.6	36.7	26.5	13.8	13.9	5.93	8.19	14.2	14.3	6.41	8.86

TABLE II: Parameters of the communication networks.

Levels	Bandwidth	Data Rate	Background Traffic
High Speed	20 Mbps	25 frames/s	RTU, Video Stream
Medium Speed	5 Mbps	25 frames/s	RTU, Video Stream
Low Speed	1 Mbps	25 frames/s	N/A

TABLE III: Mean delays of the communication networks.

Levels	High Speed	Medium Speed	Low Speed
TS-VPP	0.1 s	0.5 s	1.0 s
DS-VPP	0.05 s	0.1 s	0.2 s

the distribution and connected to the transmission system through a single point of common coupling. On the other hand, as expected, the frequency control of VPPs can effectively contribute to improve the frequency response of the system. The TS-VPP with coordinated control of DERs and ESSs has, in general, a better performance than the DS-VPP. Moreover, the geographical scattering of the resources of the TS-VPP makes the TS-VPPs outperform the DS-VPPs with respect to the reduction of the dynamic impact of communication delays.

Future work will focus on improving the coordinated control of DERs and ESSs to minimize the impact of noise and delays. We also aim at defining the minimum technical requirements that TS-VPPs and DS-VPPs have to satisfy in order to provide an adequate frequency containment support for the grid.

REFERENCES

[1] N. D. Hatziargyriou, Ed., *Microgrids – Architecture and Control*. John Wiley & Sons, 2013.

[2] Y. Liu, H. Xin, Z. Wang, and D. Gan, "Control of virtual power plant in microgrids: a coordinated approach based on photovoltaic systems and controllable loads," *IET Generation, Transmission & Distribution*, vol. 9, no. 10, pp. 921–928, 2015.

[3] M. Vasirani, R. Kota, R. L. Cavalcante, S. Ossowski, and N. R. Jennings, "An agent-based approach to virtual power plants of wind power generators and electric vehicles," *IEEE Transactions on Smart Grid*, vol. 4, no. 3, pp. 1314–1322, 2013.

[4] T. Sikorski *et al.*, "A case study on distributed energy resources and energy-storage systems in a virtual power plant concept: Technical aspects," *Energies*, vol. 13, no. 12, p. 3086, 2020.

[5] R. A. Ahangar and A. Sheykholeslami, "Bulk virtual power plant, a novel concept for improving frequency control and stability in presence of large scale res," *International Journal of Mechatronics, Electrical and Computer Technology*, vol. 4, no. 10, pp. 1017–1044, 2014.

[6] A. Oudalov, D. Chartouni, and C. Ohler, "Optimizing a battery energy storage system for primary frequency control," *IEEE Transactions on power systems*, vol. 22, no. 3, pp. 1259–1266, 2007.

[9] S. Riaz and P. Mancarella, "On feasibility and flexibility operating regions of virtual power plants and tso/dso interfaces," in *Proceedings on the 2019 IEEE Milan PowerTech*, 2019, pp. 1–6.

[7] G. Delille, B. Francois, and G. Malarange, "Dynamic frequency control support by energy storage to reduce the impact of wind and solar generation on isolated power system's inertia," *IEEE Transactions on sustainable energy*, vol. 3, no. 4, pp. 931–939, 2012.

[8] N. Etherden, V. Vyatkin, and M. H. Bollen, "Virtual power plant for grid services using iec 61850," *IEEE Transactions on Industrial Informatics*, vol. 12, no. 1, pp. 437–447, 2015.

[10] B. C. Pal, A. H. Coonick, and D. C. Macdonald, "Robust damping controller design in power systems with superconducting magnetic energy storage devices," *IEEE Transactions on Power Systems*, vol. 15, no. 1, pp. 320–325, 2000.

[11] Á. Ortega and F. Milano, "Design of a control limiter to improve the dynamic response of energy storage systems," in *2015 IEEE Power & Energy Society General Meeting*. IEEE, 2015, pp. 1–5.

[12] B. Tamimi, C. Cañizares, and K. Bhattacharya, "Modeling and performance analysis of large solar photo-voltaic generation on voltage stability and inter-area oscillations," in *Proceedings of the 2011 IEEE Power & Energy Society General Meeting*. IEEE, 2011, pp. 1–6.

[13] J. Morren, S. W. De Haan, W. L. Kling, and J. Ferreira, "Wind turbines emulating inertia and supporting primary frequency control," *IEEE Transactions on Power Systems*, vol. 21, no. 1, pp. 433–434, 2006.

[14] W. Zhong, M. A. A. Murad, M. Liu, and F. Milano, "Impact of virtual power plants on power system short-term transient response," *Electric Power Systems Research*, vol. 189, p. 106609, 2020.

[15] B. Naduvathuparambil, M. C. Valenti, and A. Feliachi, "Communication delays in wide area measurement systems," in *Proceedings of the 34th Southeastern Symposium on System Theory*. IEEE, 2002, pp. 118–122.

[16] M. Liu, I. Dassios, G. Tzounas, and F. Milano, "Stability analysis of power systems with inclusion of realistic-modeling WAMS delays," *IEEE Transactions on Power Systems*, vol. 34, no. 1, pp. 627–636, 2019.

[17] G. F. Riley and T. R. Henderson, *The ns-3 Network Simulator*. Berlin, Heidelberg: Springer Berlin Heidelberg, 2010, pp. 15–34.

[18] F. Milano, "A Python-based software tool for power system analysis," in *Proceedings of the 2013 IEEE Power & Energy Society General Meeting*. IEEE, 2013, pp. 1–5.

[19] W. Zhong, M. Liu, and F. Milano, "A co-simulation framework for power systems and communication networks," in *Proceedings of the 2019 IEEE Milan PowerTech*. IEEE, 2019, pp. 1–6.

[20] G. M. Jónsdóttir and F. Milano, "Data-based continuous wind speed models with arbitrary probability distribution and autocorrelation," *Renewable Energy*, 2019.

[21] F. Milano and R. Zárate-Miñano, "A systematic method to model power systems as stochastic differential algebraic equations," *IEEE Transactions on Power Systems*, vol. 28, no. 4, pp. 4537–4544, 2013.

[22] R. Zárate-Minano, F. M. Mele, and F. Milano, "Sde-based wind speed models with weibull distribution and exponential autocorrelation," in *Proceedings of the 2016 IEEE Power & Energy Society General Meeting*. IEEE, 2016, pp. 1–5.

[23] G. M. Jónsdóttir and F. Milano, "Modeling solar irradiance for short-term dynamic analysis of power systems," in *Proceedings of the 2019 IEEE Power & Energy Society General Meeting*. IEEE, 2019, pp. 1–5.

[24] F. Milano and M. Anghel, "Impact of time delays on power system stability," *IEEE Transactions on Circuits and Systems I: Regular Papers*, vol. 59, no. 4, pp. 889–900, 2011.

[25] P. W. Sauer and M. A. Pai, *Power System Dynamics and Stability*. Prentice hall Upper Saddle River, NJ, 1998, vol. 101.

[26] C. Murphy and A. Keane, "Local and remote estimations using fitted polynomials in distribution systems," *IEEE Transactions on Power Systems*, vol. 32, no. 4, pp. 3185–3194, 2016.